

B_c Exclusive Decays to Charmonium and a Light Meson at Next-to-Leading Order Accuracy

Cong-Feng Qiao^{a*}, Peng Sun^{b,c†}, Deshan Yang^{a‡}, and Rui-Lin Zhu^{a§}

^a Department of Physics, University of Chinese Academy of Sciences
YuQuan Road 19A, Beijing 100049, China

^b Center for High-Energy Physics, Peking University, Beijing 100871, China

^c Nuclear Science Division, LBNL, Berkeley, CA 94720, USA

Abstract

In this paper the next-to-leading order (NLO) corrections to B_c meson exclusive decays to S-wave charmonia and light pseudoscalar or vector mesons, i.e. π , K , ρ , and K^* , are performed within non-relativistic (NR) QCD approach. The non-factorizable contribution is included, which is absent in traditional naive factorization (NF). And the theoretical uncertainties for their branching ratios are reduced compared with that of direct tree level calculation. Numerical results show that NLO QCD corrections markedly enhance the branching ratio with a K factor of 1.75 for $B_c^\pm \rightarrow \eta_c \pi^\pm$ and 1.31 for $B_c^\pm \rightarrow J/\psi \pi^\pm$. In order to investigate the asymptotic behavior, the analytic form is obtained in the heavy quark limit, i.e. $m_b \rightarrow \infty$. We note that annihilation topologies contribute trivially in this limit, and the corrections at leading order in $z = m_c/m_b$ expansion come from form factors and hard spectator interactions. At last, some related phenomenologies are also discussed.

PACS numbers 12.38.Bx, 12.39.St, 13.20.He

*E-mail: qiaocf@ucas.ac.cn

†E-mail: sunp@pku.edu.cn

‡E-mail: yangds@ucas.ac.cn

§E-mail: zhuruilin09@mails.ucas.ac.cn

1 Introduction

B_c and its excited states construct the unique meson family containing two different kinds of heavy flavor. The studies on production and decay of B_c can shed light on the understanding of the strong interaction in such a unique system. In contrast to other bottom mesons just embodying one heavy flavor which can be produced remarkably through the e^+e^- and ep collisions, the cross section of B_c is suppressed owing to the associated production of two additional heavy quarks c and \bar{b} [1]. Thus massive B_c events can but refer to the hadron colliders.

After the first discovery of B_c was reported by the CDF collaboration at Tevatron in 1998 [2], there are continuous measurements of its mass in different detectors via two different channels: $B_c^\pm \rightarrow J/\psi \ell^\pm \nu_\ell$ [3, 4] and $B_c^\pm \rightarrow J/\psi \pi^\pm$ [5, 6]. Especially for the latter exclusive two-body decay, it takes advantage of a large trigger efficiency. Using this channel, the LHCb collaboration have measured the B_c mass with $6273.7 \pm 1.3(stat) \pm 1.6(sys) \text{MeV}/c^2$ recently [7]. However, the exact value of branching ratio for either $B_c^\pm \rightarrow J/\psi \ell^\pm \nu_\ell$ or $B_c^\pm \rightarrow J/\psi \pi^\pm$ has not been measured yet. And more channels should be involved to investigate the intrinsic properties of B_c . Up to now, the LHCb collaboration have successfully observed more channels beyond the two kinds in question. And they have measured the new channels $B_c^+ \rightarrow J/\psi \pi^+ \pi^- \pi^+$ [8], $B_c^\pm \rightarrow J/\psi K^\pm$ [9], $B_c^\pm \rightarrow \Psi(2S) \pi^\pm$ [10], and $B_c^\pm \rightarrow J/\psi D_s^\pm$ [11] for the first time. The study of decay properties of B_c from a multitude of processes can help us to understand the quark flavor mixing and provide precision determination of the CKM matrix parameters. Besides, according to Refs [12–14], the cross section of B_c is expected to $\sim 40 \text{nb}$ at the pp center-of-mass energy $\sqrt{s} = 14 \text{TeV}$. That means around 10^{10} B_c meson per year can be anticipated at LHC. Thus one should expect a more variety of decay channels of B_c can be measured in the upcoming experiment.

Theoretically, the exclusive two-body decay of the bottom meson is studied within the frame of the naive factorization, potential model, pQCD method and QCD factorization in the heavy quark limit. Along with the technique for the QCD factorization for the exclusive hard processes, such as π electromagnetic form-factors at the large momentum transfer and B meson decays to two light mesons, many theorists believe that the QCD factorization for $B_c^- \rightarrow J/\psi \pi^-$ holds in the heavy quark limit generally. However, there is no complete or consistent predictions based at NLO in α_s so far.

Since B_c^- contains two kinds of heavy quark, namely b and c quarks, the heavy quark limit may be realized in NRQCD approach. Therein one lets $m_b, m_c \rightarrow \infty$ and keeps the ratio $z \equiv m_c/m_b$ fixed. Then the decay amplitude of $B_c^- \rightarrow J/\psi(\eta_c) \pi^-$ is conjectured to be factorized

$$A(B_c^- \rightarrow J/\psi(\eta_c) \pi^-) \sim \Psi_{c\bar{c}}(0) \Psi_{b\bar{c}}(0) \int_0^1 dx T_H(x, \mu) \phi_\pi(x, \mu) + \mathcal{O}(1/m_b) + \mathcal{O}(v^2). \quad (1)$$

Here $\Psi_{c\bar{c}}(0)$ and $\Psi_{b\bar{c}}(0)$ denote the Schrödinger wave functions at origin of $J/\psi(\eta_c)$ and B_c^- , respectively; $T_H(x, \mu)$ is the perturbatively calculable hard kernel; and $\phi_\pi(x, \mu)$ is the Pion's light-cone distribution amplitude (LCDA).

The rough arguments of the validity of the above factorization are: 1) the energetic Pion ejected from the heavy quark system, cannot sense the surrounded soft and collinear gluons, due to the ‘‘color-transparency’’ at the leading order of heavy quark expansion, the hadronization of the collinear quark pair into a Pion is totally described by the leading twist LCDA of Pion, as the case in $B \rightarrow \pi\pi$; 2) the charm-quark in B_c needs a large momentum transfer (typically $q^2 \sim m_b m_c \sim 6 \text{GeV}^2$) to speed up for catching another energetic charm-quark from the $b \rightarrow c$ weak transition to form a quarkonia. This large momentum transfer guarantees the necessary condition for the implementation of the perturbative QCD in this process, i.e. the transition from B_c to $J/\psi(\eta_c)$ at the large recoil can be described the hard-gluon exchange, and the hadronization is to be described by the non-relativistic wave functions (at the origin) of B_c and $J/\psi(\eta_c)$, as what done in many NRQCD factorization for the exclusive quarkonia processes.

In this paper, we will adopt the factorization formula (1) to calculate $B_c \rightarrow J/\psi(\eta_c)\pi$ to the next-to-leading order of strong coupling α_s . In our calculation, we do find that all the low-energy divergences, including soft, collinear and Coulomb divergences, are either cancelled with each other (for the soft interactions), or separated with each other to be absorbed into the LCDA and the wave functions. Thus, our work can be treated as a proof for the factorization formula (1) at one-loop level.

The following sections are organized as follows: in Sect. 2 we present a brief overview of the effective weak Hamiltonian; and in Sect. 3 we present the detailed computation in the NR factorization scheme, we also deliver the asymptotic behavior in the limit $z = m_c/m_b \rightarrow 0$; in Sect. 4 we implement our results to make some phenomenological predictions for the branching ratios of various B_c two-body decays to a S-wave quarkonium and a light meson, and some detailed discussions are also presented; at last we conclude in Sect. 5.

2 The theoretical frame

In the Standard Model (SM), $B_c^- \rightarrow J/\psi\pi^-$ occurs through W -mediated charge current process. However, since $m_W \gg m_{b,c}$, Λ_{QCD} , the large logarithm arise in the higher order strong interaction corrections. Thus, the RG-improved perturbation theory must be resorted. In the community of B physics, this turns to be the effective weak Hamiltonian method. The effective weak Hamiltonian governing $B_c^- \rightarrow J/\psi\pi^-$ is

$$\mathcal{H}_{\text{eff}} = \frac{G_F}{\sqrt{2}} V_{ud}^* V_{cb} (C_1(\mu) Q_1(\mu) + C_2(\mu) Q_2(\mu)) , \quad (2)$$

with G_F being the Fermi constants, V_{ud} and V_{cb} the Cabibbo-Kobayashi-Maskawa (CKM) matrix-elements, $C_{1,2}(\mu)$ the perturbatively calculable Wilson coefficients, and $Q_{1,2}(\mu)$ the effective four-quark operators

$$Q_1 = \bar{d}_\alpha \gamma^\mu (1 - \gamma_5) u_\alpha \bar{c}_\beta \gamma_\mu (1 - \gamma_5) b_\beta , \quad (3a)$$

$$Q_2 = \bar{d}_\alpha \gamma^\mu (1 - \gamma_5) u_\beta \bar{c}_\beta \gamma_\mu (1 - \gamma_5) b_\alpha , \quad (3b)$$

where α, β are color indices and the summation convention over repeated indices are understood. For the conveniences of our later calculations, we will adopt another operator basis, i.e.

$$Q_0 = \bar{d}_\alpha \gamma^\mu (1 - \gamma_5) u_\alpha \bar{c}_\beta \gamma_\mu (1 - \gamma_5) b_\beta , \quad (4a)$$

$$Q_8 = \bar{d}_\alpha T_{\alpha\beta}^A \gamma^\mu (1 - \gamma_5) u_\beta \bar{c}_\rho T_{\rho\lambda}^A \gamma_\mu (1 - \gamma_5) b_\lambda , \quad (4b)$$

where T^A s are the generators of the fundamental representation for $\text{SU}_C(3)$. Applying the Fierz rearrangement relation

$$T_{\alpha\beta}^A T_{\rho\lambda}^A = -\frac{1}{6} \delta_{\alpha\beta} \delta_{\rho\lambda} + \frac{1}{2} \delta_{\alpha\lambda} \delta_{\rho\beta} , \quad (5)$$

we have immediately

$$Q_0 = Q_1 , \quad Q_8 = -\frac{1}{6} Q_1 + \frac{1}{2} Q_2 . \quad (6)$$

Consequently, for the Wilson coefficients, we have

$$C_0 = C_1 + C_2/3 , \quad C_8 = 2C_2 . \quad (7)$$

Then, the decay amplitude of $B_c^- \rightarrow J/\psi(\eta_c)\pi^-$ can be written as

$$\begin{aligned} \mathcal{A}(B_c^- \rightarrow J/\psi(\eta_c)\pi^-) &= \langle J/\psi(\eta_c)\pi^- | \mathcal{H}_{\text{eff}} | B_c^- \rangle \\ &= \frac{G_F}{\sqrt{2}} V_{ud}^* V_{cb} (C_0(\mu) \langle Q_0(\mu) \rangle + C_8(\mu) \langle Q_8(\mu) \rangle) . \end{aligned} \quad (8)$$

3 The non-relativistic approach

Systematically, the non-relativistic QCD effective theory provides an rigorous factorization formalism for the annihilation and production of heavy quarkonia [15]. In this framework, the heavy quarkonium's production comes from two steps: a Fock state such as $|q\bar{q}\rangle$, $|q\bar{q}g\rangle$ produced at short-distance by a large momentum transfer process, followed by it binding to quarkonium at long-distance.

In the process of $B_c^- \rightarrow J/\psi(\eta_c)\pi^-$, all the non-perturbative binding effects are attributed to three factors: Pion decay constant and the Schrödinger wave functions at origin of $J/\psi(\eta_c)$ and B_c . While the hard kernel can be calculated perturbatively.

3.1 LO

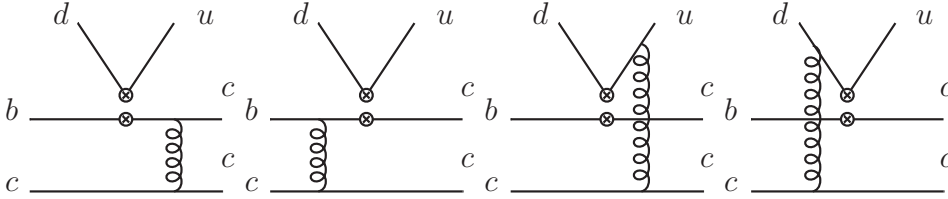


Figure 1: The quark-level Feynman diagrams at leading order for $B_c \rightarrow J/\psi(\eta_c)\pi$. The 4-vertex “ $\otimes \otimes$ ” denotes the insertion of a 4-fermion operator Q_i .

The possible quark-level topologies for $B_c \rightarrow J/\psi(\eta_c)\pi$ are portrayed in Figure 1, where we assign momentum xP to the u-quark and $(1-x)P$ to the d-quark in the emitted Pion. The former two in Figure 1 contribute to $\langle Q_0 \rangle$, and the others contribute to $\langle Q_8 \rangle$. It is completely perturbatively calculable sector. Associated with non-perturbative parameters: Pion decay constant and the Schrödinger wave functions at origin of $J/\psi(\eta_c)$ and B_c , we have the tree-level $\langle Q_i \rangle$, leaving the momentum fraction x unintegrated

$$\begin{aligned} \langle Q_0(\eta_c) \rangle_x &= \frac{8\sqrt{2}\pi f_\pi \psi_{\eta_c}(0) \psi_{B_c}(0) \phi_\pi(x) C_A C_F \alpha_s \sqrt{m_b + m_c} (m_b + 3m_c) (2m_b m_c + 3m_b^2 + 3m_c^2)}{m_c^{3/2} N_c (m_b - m_c)^3}, \\ \langle Q_8(\eta_c) \rangle_x &= \frac{2\sqrt{2}\pi f_\pi \psi_{\eta_c}(0) \psi_{B_c}(0) \phi_\pi(x) C_A C_F \alpha_s \sqrt{m_b + m_c} (m_b + 3m_c)^2 (xm_c - (x-1)m_b)}{m_c^{3/2} N_c^2 (m_c - m_b) ((x-1)m_b + (3x-2)m_c) (xm_b + (3x-1)m_c)}, \end{aligned} \quad (9)$$

where more detail about f_π , $\psi_{\eta_c}(0)$, $\psi_{B_c}(0)$, and Pion light cone distribution amplitude $\phi_\pi(x, \mu)$ can be found in Appendix A. Note that higher twist contribution comes from twist-4. Referring to J/ψ , the corresponding matrix elements are

$$\begin{aligned} \langle Q_0(J/\psi) \rangle_x &= -\frac{64\sqrt{2}\pi f_\pi \psi_{J/\psi}(0) \psi_{B_c}(0) \phi_\pi(x) P_{B_c} \cdot \varepsilon_\Psi^* C_A C_F \alpha_s (m_b + m_c)^{5/2}}{m_c^{1/2} N_c (m_b - m_c)^4}, \\ \langle Q_8(J/\psi) \rangle_x &= -\frac{8\sqrt{2}\pi f_\pi \psi_{J/\psi}(0) \psi_{B_c}(0) \phi_\pi(x) P_{B_c} \cdot \varepsilon_\Psi^* C_A C_F \alpha_s (m_b + m_c)^{1/2}}{m_c^{1/2} N_c^2 (m_b - m_c)^2 ((x-1)m_b + (3x-2)m_c) (xm_b + (3x-1)m_c)} \\ &\quad \times (3(2x-1)m_b m_c + (x-1)m_b^2 + (9x-4)m_c^2). \end{aligned} \quad (10)$$

Note that $\langle Q_8 \rangle$ in Equation (9) and (10) is not symmetrical when exchange x with $\bar{x} = 1 - x$, because of the non-factorizable contribution from axial vector current which brings in an anti-symmetrical part. However, the anti-symmetrical part can be easily proved to be insignificant. We define the function $V(x)$ to collect the contributions from axial vector current, and it satisfies $V(\bar{x}) = -V(x)$. Considering the symmetrical Pion LCDA, i.e. $\phi_\pi(\bar{x}) = \phi_\pi(x)$, we can get the result

$$\int_0^1 V(x) \phi_\pi(x) dx = -\int_1^0 V(\bar{x}) \phi_\pi(\bar{x}) dx = -\int_0^1 V(x) \phi_\pi(x) dx = 0. \quad (11)$$

Employing the asymptotic LCDA $\phi_\pi(x, \mu \rightarrow \infty) = 6x\bar{x}$, we can obtain the integrated matrix elements $\langle Q_i \rangle$

$$\begin{aligned}
\langle Q_0(\eta_c) \rangle &= \frac{8\sqrt{2}\pi f_\pi \psi_{\eta_c}(0) \psi_{B_c}(0) C_A C_F \alpha_s \sqrt{m_b + m_c} (m_b + 3m_c) (2m_b m_c + 3m_b^2 + 3m_c^2)}{m_c^{3/2} N_c (m_b - m_c)^3}, \\
\langle Q_8(\eta_c) \rangle &= \frac{6\sqrt{2}\pi f_\pi \psi_{\eta_c}(0) \psi_{B_c}(0) C_A C_F \alpha_s \sqrt{m_b + m_c}}{m_c^{3/2} N_c^2 (m_b - m_c) (m_b + 3m_c)} \times [2m_b m_c (\ln(m_b + 2m_c) \\
&\quad - \ln(m_c) + 2) + m_c^2 (4 \ln(m_b + 2m_c) - 4 \ln(m_c) + 3) + m_b^2], \\
\langle Q_0(\Psi) \rangle &= -\frac{64\sqrt{2}\pi f_\pi \psi_{J/\psi}(0) \psi_{B_c}(0) P_{B_c} \cdot \varepsilon_\Psi^* C_A C_F \alpha_s (m_b + m_c)^{5/2}}{m_c^{1/2} N_c (m_b - m_c)^4}, \\
\langle Q_8(\Psi) \rangle &= -\frac{24\sqrt{2}\pi f_\pi \psi_{J/\psi}(0) \psi_{B_c}(0) P_{B_c} \cdot \varepsilon_\Psi^* C_A C_F \alpha_s (m_b + m_c)^{1/2} \times [2m_b m_c (\ln(m_b + 2m_c) \\
&\quad - \ln(m_c) + 2) + m_c^2 (4 \ln(m_b + 2m_c) - 4 \ln(m_c) + 3) + m_b^2]}{m_c^{1/2} N_c^2 (m_b - m_c) (m_b + 3m_c)^3}. \tag{12}
\end{aligned}$$

Rather than the traditional formalisms in Refs. [16, 17], herein we extracted hard kernels T_i from Wilson coefficients separately. They can be calculated perturbatively order by order.

$$\mathcal{A}(B_c^- \rightarrow J/\psi(\eta_c)\pi^-) = \frac{G_F}{\sqrt{2}} V_{ud}^* V_{cb} (C_0(\mu) T_{f,0} M_f + C_0(\mu) T_{nf,0} M_{nf} + C_8(\mu) T_{nf,8} M_{nf}), \tag{13}$$

$$T_{f,i}(\mu) = \sum_{k=0}^{\infty} \left(\frac{\alpha_s}{4\pi}\right)^k T_{f,i}^{(k)}(\mu), \quad T_{nf,i}(\mu) = \sum_{k=0}^{\infty} \left(\frac{\alpha_s}{4\pi}\right)^k T_{nf,i}^{(k)}(\mu), \tag{14}$$

where T_f means factorizable hard kernel, T_{nf} means non-factorizable hard kernel. And the Wilson coefficients C_i are

$$C_0 = \frac{2}{3} C_+ + \frac{1}{3} C_-, \quad C_8 = C_+ - C_-, \tag{15}$$

where

$$C_\pm = \left[\frac{\alpha_s(M_W)}{\alpha_s(\mu)} \right]^{\frac{\gamma_\pm}{2\beta_0}}, \quad \gamma_\pm = \pm 6 \frac{N_c \mp 1}{N_c}, \quad \beta_0 = \frac{11N_c - 2n_f}{3}. \tag{16}$$

Fixing $M_f(\eta_c) = \langle Q_0(\eta_c) \rangle$, $\bar{M}_f(J/\psi) = \langle Q_0(\Psi) \rangle$, $M_{nf}(\eta_c) = \langle Q_8(\eta_c) \rangle$ and $M_{nf}(J/\psi) = \langle Q_8(\Psi) \rangle$, we can extract the leading order hard kernel $T_i^{(0)}$

$$T_{f,0}^{(0)}(\eta_c) = T_{f,0}^{(0)}(J/\psi) = 1, \quad T_{nf,0}^{(0)}(\eta_c) = T_{nf,0}^{(0)}(J/\psi) = 0, \quad T_{nf,8}^{(0)}(\eta_c) = T_{nf,8}^{(0)}(J/\psi) = 1. \tag{17}$$

3.2 NLO

Now we pay more attention to the corrections at next-to-leading order. The one loop diagrams for $B_c \rightarrow J/\psi(\eta_c)\pi$ are classified into Figures 2, 3 and 4. Where Fig. 2 lays out the one loop factorizable diagrams while non-factorizable diagrams are shown in Figs 3 and 4. To regularize the Ultra-Violet and Infra-Red divergences we use dimensional regularization scheme, but relative velocity regularization scheme for Coulomb divergence. The renormalization constants are listed in Appendix B. In our calculation, the Mathematical package FeynArts [18] was used to generate the Feynman diagrams, FeynCalc [19] to deal with the amplitudes, and LoopTools [20] to calculate the one-loop integrals. The practicable γ_5 -scheme is adopted in D dimensional computation [21, 22].

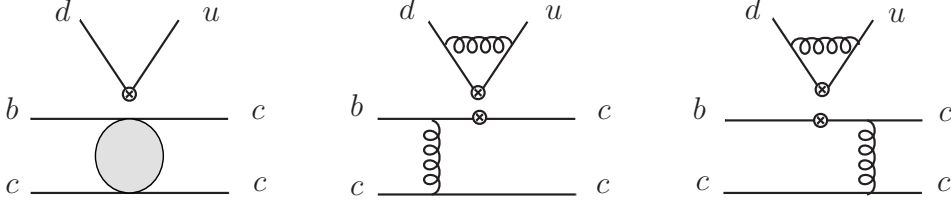


Figure 2: One loop factorizable diagrams contribute to $\langle Q_0 \rangle$. The bubble in the first diagram expresses all one loop form factor diagrams, which are displayed in Refs [25, 27].

3.2.1 $T_0^{(1)}$

The one loop diagrams contribute to $\langle Q_0 \rangle$ can be distributed into two sets: factorizable (see Fig. 2) and non-factorizable (see Fig. 3). And the NLO B_c -to-S-wave-charmonium form factors have been calculated in Refs [25–28]. For the rear two in Fig. 2, their UV divergence can be canceled by external field counter terms.

We analyzed the factorizable part at first. In NF, $\langle Q_8 \rangle$ vanishes, and

$$\langle J/\psi(\eta_c)\pi^-|Q_0|B_c^- \rangle \approx \langle J/\psi(\eta_c)|\bar{c}\gamma^\mu(1-\gamma_5)b|B_c^- \rangle \langle \pi^-|\bar{d}\gamma_\mu(1-\gamma_5)u|0 \rangle, \quad (18)$$

i.e. $\langle Q_0 \rangle$ is proportional to the product of the Pion decay constant and $B_c^- \rightarrow J/\psi(\eta_c)$ transition form-factor. Conventionally, we adopt the following parameterizations for the decay constants and $B_c^- \rightarrow J/\psi(\eta_c)$ transition form-factors

$$\langle \eta_c(p)|\bar{c}\gamma_\mu\gamma_5c|0 \rangle = -if_{\eta_c}p_\mu, \quad (19)$$

$$\langle \pi^-(p')|\bar{d}\gamma_\mu\gamma_5u|0 \rangle = -if_\pi p'_\mu, \quad (20)$$

$$\langle B_c^-(P)|\bar{c}\gamma_\mu\gamma_5b|0 \rangle = -if_{B_c}P_\mu, \quad (21)$$

$$\langle J/\psi(p, \varepsilon^*)|\bar{c}\gamma_\mu c|0 \rangle = -if_{J/\psi}m_{J/\psi}\varepsilon_\mu^*, \quad (22)$$

$$\langle \eta_c(p)|\bar{c}\gamma^\mu b|B_c^-(P) \rangle = f_+(q^2) \left[P^\mu + p^\mu - \frac{m_{B_c}^2 - m_{\eta_c}^2}{q^2} q^\mu \right] + f_0(q^2) \frac{m_{B_c}^2 - m_{\eta_c}^2}{q^2} q^\mu, \quad (23)$$

$$\langle \eta_c(p)|\bar{c}\gamma^\mu\gamma_5b|B_c^-(P) \rangle = 0, \quad (24)$$

$$\langle J/\psi(p, \varepsilon^*)|\bar{c}\gamma^\mu b|B_c^-(P) \rangle = \frac{2iV(q^2)}{m_{B_c} + m_{J/\psi}} \epsilon^{\mu\nu\rho\sigma} \varepsilon_\nu^* p_\rho P_\sigma, \quad (25)$$

$$\begin{aligned} \langle J/\psi(p, \varepsilon^*)|\bar{c}\gamma^\mu\gamma_5b|B_c^-(P) \rangle &= 2m_{J/\psi}A_0(q^2) \frac{\varepsilon^* \cdot q}{q^2} q^\mu + (m_{B_c} + m_{J/\psi})A_1(q^2) \left[\varepsilon^{*\mu} - \frac{\varepsilon^* \cdot q}{q^2} q^\mu \right] \\ &\quad - A_2(q^2) \frac{\varepsilon^* \cdot q}{m_{B_c} + m_{J/\psi}} \left[P^\mu + p^\mu - \frac{m_{B_c}^2 - m_{J/\psi}^2}{q^2} q^\mu \right], \end{aligned} \quad (26)$$

here we define momentum transfer $q = P - p$ and $\epsilon^{0123} = -1$. Note that $f_0(0) = f_+(0)$.

The tree-level form factors can be obtained easily. They read

$$f_+^{LO}(q^2) = \frac{8\sqrt{2}C_A C_F \pi \sqrt{z+1} \left(-\frac{q^2}{m_b^2} + 3z^2 + 2z + 3 \right) \alpha_s \psi(0)_{B_c} \psi(0)_{\eta_c}}{\left(\frac{q^2}{m_b^2} - (z-1)^2 \right)^2 z^{3/2} m_b^3 N_c}, \quad (27)$$

$$f_0^{LO}(q^2) = \frac{8\sqrt{2}C_A C_F \pi \sqrt{z+1} \left(9z^3 + 9z^2 + 11z - \frac{q^2}{m_b^2} (5z+3) + 3 \right) \alpha_s \psi(0)_{B_c} \psi(0)_{\eta_c}}{\left(\frac{q^2}{m_b^2} - (z-1)^2 \right)^2 z^{3/2} (3z+1) m_b^3 N_c}, \quad (28)$$

$$V^{LO}(q^2) = \frac{16\sqrt{2}C_A C_F \pi (3z+1) \alpha_s \psi(0)_{B_c} \psi(0)_{J/\psi}}{\left(\frac{q^2}{m_b^2} - (z-1)^2\right)^2 \left(\frac{z}{z+1}\right)^{3/2} m_b^3 N_c}, \quad (29)$$

$$A_0^{LO}(q^2) = \frac{16\sqrt{2}C_A C_F \pi (z+1)^{5/2} \alpha_s \psi(0)_{B_c} \psi(0)_{J/\psi}}{\left(\frac{q^2}{m_b^2} - (z-1)^2\right)^2 z^{3/2} m_b^3 N_c}, \quad (30)$$

$$A_1^{LO}(q^2) = \frac{16\sqrt{2}C_A C_F \pi \sqrt{z+1} \left(4z^3 + 5z^2 + 6z - \frac{q^2}{m_b^2}(2z+1) + 1\right) \alpha_s \psi(0)_{B_c} \psi(0)_{J/\psi}}{\left(\frac{q^2}{m_b^2} - (z-1)^2\right)^2 z^{3/2} (3z+1) m_b^3 N_c}, \quad (31)$$

$$A_2^{LO}(q^2) = \frac{16\sqrt{2}C_A C_F \pi \sqrt{z+1} (3z+1) \psi(0)_{B_c} \psi(0)_{J/\psi}}{\left(\frac{q^2}{m_b^2} - (z-1)^2\right)^2 z^{3/2} m_b^3 N_c}, \quad (32)$$

here, $z \equiv m_c/m_b$.

When neglecting the mass of Pion, we have the factorizable contribution in NF

$$\begin{aligned} \langle \eta_c \pi^- | Q_{0,f} | B_c^- \rangle &= i f_\pi f_0(0) (m_{B_c}^2 - m_{\eta_c}^2), \\ \langle J/\psi \pi^- | Q_{0,f} | B_c^- \rangle &= -i f_\pi A_0(0) (m_{B_c}^2 - m_{J/\psi}^2), \end{aligned} \quad (33)$$

where we have used the fact that J/ψ is longitudinally polarized so that

$$2m_{J/\psi} \varepsilon^* \cdot P = 2m_{B_c} |\vec{p}_c| = m_{B_c}^2 - m_{J/\psi}^2.$$

Therefore we have the LO result

$$\langle \eta_c \pi^- | Q_0 | B_c^- \rangle^{LO} = i \frac{8\sqrt{2}\pi \alpha_s C_A C_F \sqrt{z+1} (9z^3 + 9z^2 + 11z + 3) f_\pi \psi(0)_{B_c} \psi(0)_{\eta_c}}{(1-z)^3 z^{3/2} m_b N_c}, \quad (34)$$

and in the heavy quark limit $z \rightarrow 0$, we have

$$\lim_{z \rightarrow 0} \langle \eta_c \pi^- | Q_0 | B_c^- \rangle^{LO} = i \frac{24\sqrt{2}\pi \alpha_s C_A C_F f_\pi \psi(0)_{B_c} \psi(0)_{\eta_c}}{z^{3/2} m_b N_c}, \quad (35)$$

Actually the approximation above is not so good. Numerically, we have

$$\left. \frac{\lim_{z \rightarrow 0} \langle \eta_c \pi^- | Q_0 | B_c^- \rangle^{LO}}{\langle \eta_c \pi^- | Q_0 | B_c^- \rangle^{LO}} \right|_{z=1.5/4.8} \approx 0.11, \quad (36)$$

which is essentially bad. The perturbative series expanded as equation (13), however, can resolve the problem. Because the convergence of hard kernel T_i is well-behaved.

Note that the complete analytic expression is too lengthy to be presented and it is possible to derive an asymptotic analytic formula valid in phenomenological application. Thus, we present our results in the heavy quark limit, i.e. $m_b \rightarrow \infty$.

The factorizable hard kernel $T_{f,0}^{(1)}$ is identical to the ratio of NLO form factor to the tree level one

$$\begin{aligned}
T_{f,0}^{(1)}(\eta_c) = \frac{f_0^{(1)}(0)}{f_0^{(0)}(0)} &= \frac{1}{3}(11C_A - 2n_f) \ln\left(\frac{2\mu^2}{zm_b^2}\right) - \frac{10n_f}{9} - \frac{1}{3} \ln z - \frac{2 \ln 2}{3} \\
&+ C_F \left(\frac{1}{2} \ln^2 z + \frac{10}{3} \ln 2 \ln z - \frac{35}{6} \ln z + \frac{2 \ln^2 2}{3} \right. \\
&\left. + 3 \ln 2 + \frac{7\pi^2}{9} - \frac{103}{6} \right) \\
&+ C_A \left(-\frac{1}{6} \ln^2 z - \frac{1}{3} \ln 2 \ln z - \frac{1}{3} \ln z + \frac{\ln^2 2}{3} \right. \\
&\left. - \frac{4 \ln 2}{3} - \frac{5\pi^2}{36} + \frac{73}{9} \right), \tag{37}
\end{aligned}$$

$$\begin{aligned}
T_{f,0}^{(1)}(\Psi) = \frac{A_0^{(1)}(0)}{A_0^{(0)}(0)} &= \frac{1}{3}(11C_A - 2n_f) \ln\left(\frac{2\mu^2}{zm_b^2}\right) - \frac{10n_f}{9} + C_F \left(\frac{1}{2} \ln^2 z - \frac{119}{8} \right. \\
&\left. + 7 \ln 2 \ln z - \frac{21}{4} \ln z + 7 \ln^2 2 + \frac{15 \ln 2}{4} \right) \\
&+ C_A \left(-\frac{3}{8} \ln^2 z - \ln 2 \ln z - \frac{9}{8} \ln z - \frac{7\pi^2}{24} + \frac{67}{9} \right. \\
&\left. - \frac{9 \ln^2 2}{4} + \frac{3 \ln 2}{8} \right). \tag{38}
\end{aligned}$$

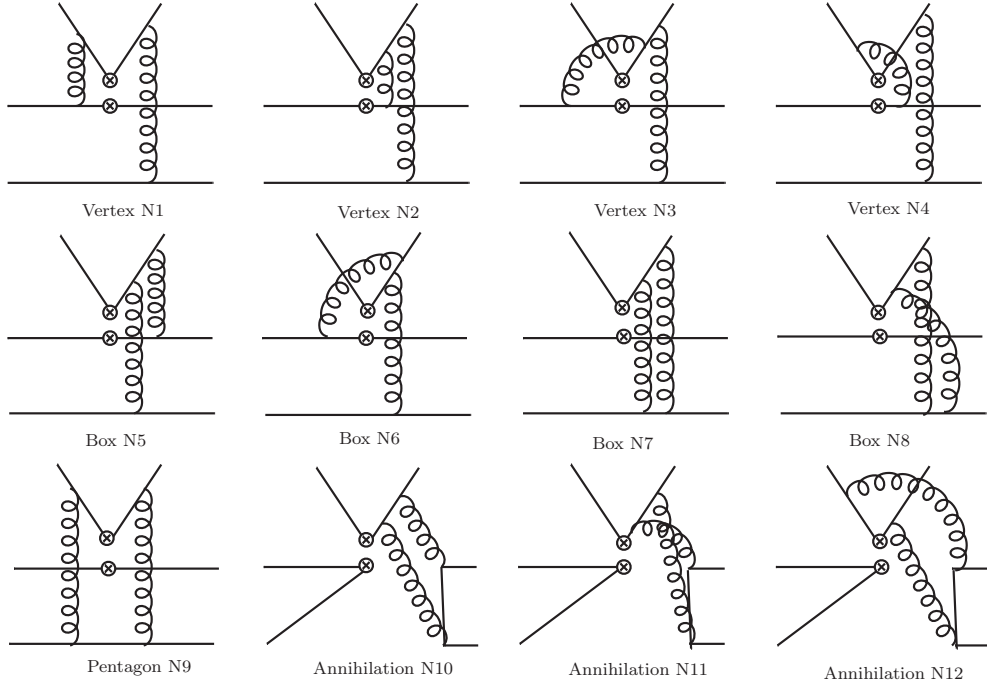


Figure 3: Twelve of twenty-four one loop non-factorizable diagrams contribute to $\langle Q_0 \rangle$. The other twelve partners can be obtained by interchanging u and d quarks.

Next, we turn to the non-factorizable part. There are twenty-four one loop non-factorizable diagrams contribute to $\langle Q_0 \rangle$, half of which are displayed in Fig. 3. The corresponding color factors are summed up in Table 1. Over one hundred of one-loop integrals in Fig. 3 and Fig. 4 are created, and they can be reduced into Master Integrals(MI) and some two-point Passarino-Veltman integrals [20]. Our analytic expressions of MI are in agreement with what given in Refs [29, 30].

Table 1: Color factors of the corresponding diagrams in Fig. 3. Therein the figures from N1 to N9, contribute not only $\langle Q_0 \rangle$, but also $\langle Q_8 \rangle$.

Diagram	N1-2,N6,N8-9	N3-5,N7	N10-12
color in $\langle Q_8 \rangle$	$\frac{(C_A^2-2)C_F}{4}$	$-\frac{C_F}{2}$	0
color in $\langle Q_0 \rangle$	$\frac{C_A C_F}{2}$		

Table 2: Color factors of the corresponding diagrams in Fig. 4. They contribute only to $\langle Q_8 \rangle$.

Diagram	N13,N15,N17-18,N27-29,N33-36	N14,N26	N16,N24-25	N19-23,N30-32
color in $\langle Q_8 \rangle$	$\frac{2C_A C_F}{3}$	$\frac{iC_A^2 C_F}{4}$	$-\frac{iC_A^2 C_F}{4}$	$-\frac{C_A C_F}{12}$

The numerical one loop non-factorizable contribution for $T_{nf,0}^{(1)}$ are

$$T_{nf,0}^{(1)}(\eta_c) = 6 \ln\left(\frac{m_b^2}{\mu^2}\right) + 16.75, \quad (39)$$

$$T_{nf,0}^{(1)}(\Psi) = T_{nf,0}^{(1)}(\eta_c). \quad (40)$$

And the complete results in heavy quark limit can be found in Appendix C.

3.2.2 $T_8^{(1)}$

Here, we study the one loop non-factorizable contributions to $\langle Q_8 \rangle$. Twenty-four diagrams are showed up in Fig. 4, another nine diagrams are collected in Fig. 3 from N1 to N9, and the rest ones can be obtained by interchanging u and d quarks. The corresponding color factors are summed up in Table 1 and Table 2.

After integrating the fraction, we have the corresponding $T_{nf,8}^{(1)}$

$$\begin{aligned} T_{nf,8}^{(1)}(\eta_c) &= \frac{1}{3} (-11C_A + 2n_f + 16N_c - 6) \ln\left(\frac{m_b^2}{\mu^2}\right) - \frac{12.48}{N_c} + (9 \ln z + 1)C_F \\ &\quad - \left(\frac{\ln^2 z}{2} - \frac{6 \ln 2 - 23}{3} \ln z + 278.1\right)C_A - \frac{2}{9}n_f(-3 \ln z + 5 + 3 \ln 2) \\ &\quad + \frac{\ln^2 z}{6} - \frac{8(3 + \ln 2)}{3} \ln z + 548.9, \end{aligned} \quad (41)$$

$$\begin{aligned} T_{nf,8}^{(1)}(\Psi) &= \frac{1}{9} (-33C_A + 6n_f + 32N_c - 18) \ln\left(\frac{m_b^2}{\mu^2}\right) - \frac{12.48}{N_c} + (9 \ln z + 1)C_F \\ &\quad - \left(\frac{\ln^2 z}{2} - \frac{6 \ln 2 - 23}{3} \ln z + 278.1\right)C_A - \frac{2}{9}n_f(-3 \ln z + 5 + 3 \ln 2) \\ &\quad + \frac{\ln^2 z}{6} - \frac{8(3 + \ln 2)}{3} \ln z + 542.3. \end{aligned} \quad (42)$$

4 The phenomenological studies

The decay width can be written as:

$$\Gamma(B_c \rightarrow J/\psi(\eta_c)\pi) = \frac{|p|}{8\pi m_{B_c}^2} |\mathcal{A}(B_c \rightarrow J/\psi(\eta_c)\pi)|^2, \quad (43)$$

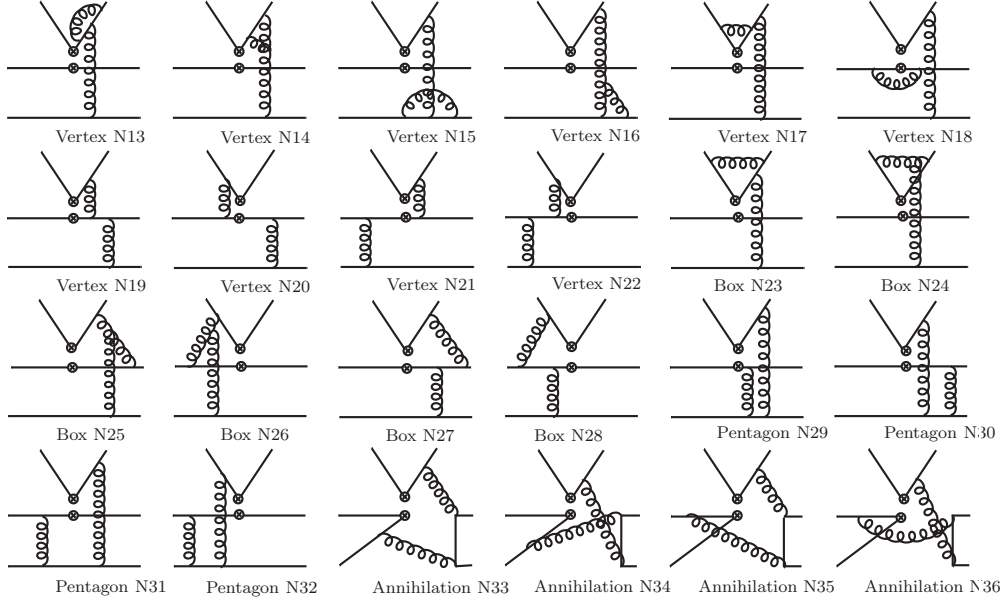


Figure 4: Twenty-four of the sixty-five one loop non-factorizable diagrams contribute to $\langle Q_8 \rangle$. Another twenty-three diagrams can be obtained by interchanging u and d quark. And the left eighteen come from the diagrams Vertex N1 to Pentagon N9 in Fig. 3 and their symmetrical partners.

here the momentum of final particle satisfies $|p| = (m_{B_c}^2 - m_\psi^2)/2m_{B_c}$ in the B_c meson rest frame, and we adopt the input parameters as below [39]

$$\begin{aligned}
m_c &= 1.4 \pm 0.1 \text{ GeV}, \quad m_b = 4.9 \pm 0.1 \text{ GeV}, \quad \Lambda_{QCD} = 100 \text{ MeV}, \quad G_F = 1.16637 \times 10^{-5} \text{ GeV}^{-2}, \\
|V_{ud}^* V_{cb}| &= A\lambda^2(1 - \lambda^2/2 - \lambda^4/8), \quad n_f = 3, \quad N_c = 3, \quad C_F = 4/3, \quad |V_{us}^*| = 0.2252, \\
|V_{cb}| &= 0.0406, \quad f_\pi = 130.4 \text{ MeV}, \quad f_\rho = 216 \text{ MeV}, \quad f_K = 156.1 \text{ MeV}, \quad f_K^* = 220 \text{ MeV},
\end{aligned}$$

where $A = 0.814$, $\lambda = 0.2257$. The Schrödinger wave function at the origin for J/ψ is determined through its leptonic decay width $\Gamma_{ee}^\psi = 5.55 \text{ keV}$ [39]. Numerically we can obtain $|\psi_\Psi^{LO}(0)|^2 = 0.0447(\text{GeV})^3$ and $|\psi_\Psi^{NLO}(0)|^2 = 0.0801(\text{GeV})^3$. For that of B_c , we shall determine its value to be: $|\psi_{B_c}(0)|^2 = 0.1307(\text{GeV})^3$, which is derived under the Buchmüller-Tye potential [40]. Besides, the one loop result for strong coupling constant is used, i.e.

$$\alpha_s(\mu) = \frac{4\pi}{(11 - \frac{2}{3}n_f) \ln(\frac{\mu^2}{\Lambda_{QCD}^2})}.$$

Within the above input parameters, we can obtain the decay width of B_c decays to S-wave charmonium and Pion at NLO accuracy. In practise, the renormalization scale μ may run from $2m_c$ to m_b , and the μ dependence of branching ratio is shown in Figure 5. Therein, we plot both kinds of NLO results: one letting $m_c/m_b \rightarrow 0$ in heavy-quark-limit; the other fixing the ratio m_c/m_b to its physical value. The first one is valid in leading m_c/m_b , while the latter summed to all orders of m_c/m_b . It turned out the leading order approximation in m_c/m_b expansion, namely Asymptotic NLO result, account for more than 85% of the complete NLO result. That means it is enough for us to use this simple and analytic expression for phenomenological studies in place of complicated NLO expression. The NLO corrections can reduce the uncertainty, which is explicitly exhibited in Figure 6.

Apart from the uncertainty of renormalization scale, we also study the uncertainty from quark mass. We found that both of them are important for the final results. The vivid figures considering both dependence are drawn in Figure 7. In which, we also detailed the influences from Gegenbauer

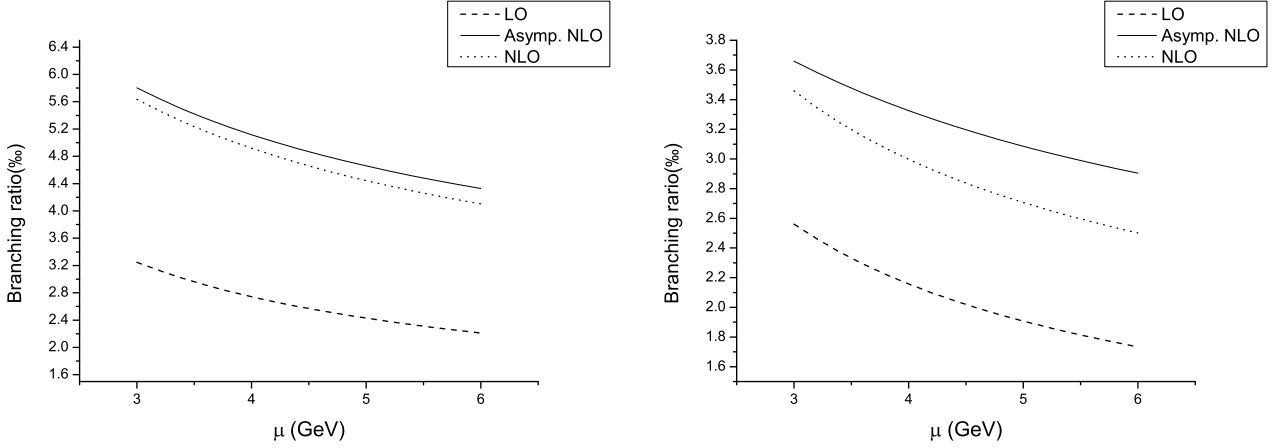


Figure 5: The branching ratios of $B_c \rightarrow \eta_c \pi$ (left) and $B_c \rightarrow J/\psi \pi$ (right) versus renormalization scale μ . Herein $m_c = 1.5\text{GeV}$, $m_b = 4.8\text{GeV}$, and for the lifetime of the B_c we take $\tau(B_c) = 0.453$ ps. The results of LO, Asymptotic NLO, and complete NLO are shown.

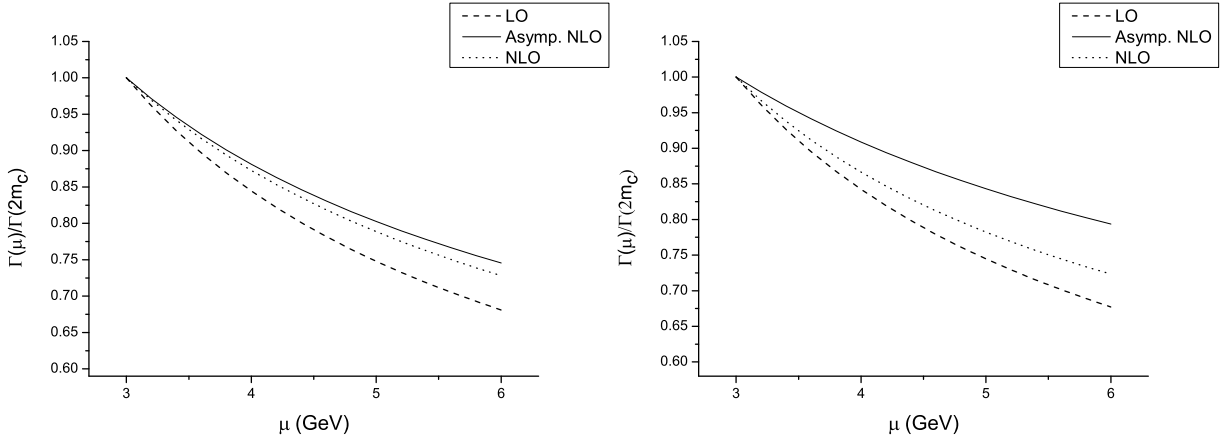


Figure 6: The ratio $\Gamma(\mu)/\Gamma(2m_c)$ of $B_c \rightarrow \eta_c \pi$ (left) and $B_c \rightarrow J/\psi \pi$ (right) versus renormalization scale μ . Herein $m_c = 1.5\text{GeV}$, $m_b = 4.8\text{GeV}$.

polynomials of light cone distribution amplitude of Pion, however, which brings about slight influence to the final result.

After considered the uncertainties stated above, we give out our results based on NR QCD factorization in Table 3 and compare them with that calculated from other models. The LO results are generally close to results of the QCD sum rule [41, 42], the constituent quark model [43, 47–49] and light-front ISGW model [44], however larger than that of the relativistic potential model [45] and the relativistic quark model [46]. Our work showed that the NLO corrections substantially enhance the branching ratios, and the NLO QCD correction K factors are, $1.75^{+0.14+0.18}_{-0.34-0.11}$ for $\Gamma(B_c \rightarrow \eta_c \pi)$ and $1.31^{+0.06+0.18}_{-0.18-0.12}$ for $\Gamma(B_c \rightarrow J/\psi \pi)$.

Moreover, we want to study the degree of importance for the factorizable part at NLO accuracy. After calculation, we found that the asymptotic factorizable contribution can be well-represented the majority of the branching ratio. To present it more vividly, let us set $m_c = 1.4\text{GeV}$, $m_b = 4.9\text{GeV}$, and $\mu = 3\text{GeV}$, and we obtain

$$\begin{aligned} Br(B_c \rightarrow \eta_c \pi)^{\text{Asymp. factorizable}} &= 5.10\%, & Br(B_c \rightarrow \eta_c \pi)^{\text{total}} &= 5.20\%, \\ Br(B_c \rightarrow J/\psi \pi)^{\text{Asymp. factorizable}} &= 3.06\%, & Br(B_c \rightarrow J/\psi \pi)^{\text{total}} &= 2.91\%. \end{aligned} \quad (44)$$

Experimentally, the pp collisions at LHC have been performed at center-of-mass energy $\sqrt{s} =$

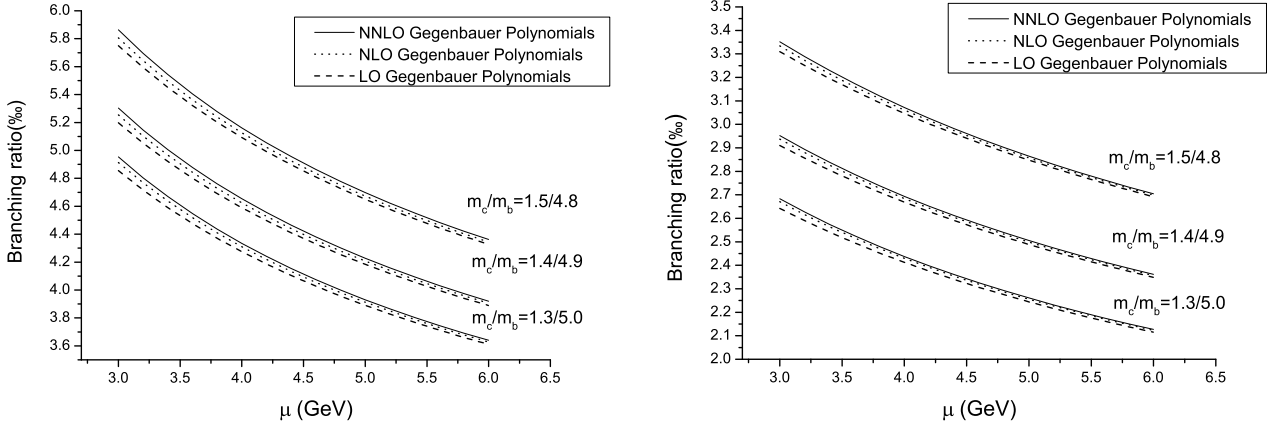


Figure 7: The branching ratio of $B_c \rightarrow \eta_c \pi$ (left) and $B_c \rightarrow J/\psi \pi$ (right) versus renormalization scale μ , for different choices of quark mass. And LO, NLO, NNLO Gegenbauer polynomials of Pion's light cone distribution amplitude are considered respectively.

8TeV. And the energy will arrive at $\sqrt{s} = 14\text{TeV}$ in the future days. pp collisions provide a mass-production source for B_c meson. Since the B_c^* decays into the B_c with a probability of almost 100%, including the contributions from the S-wave excited states, the cross section of the B_c meson at LHC was estimated to be around 10^2nb . With 10fb^{-1} of integrated luminosity, there are around 10^9 events for B_c production. Then, the measurements of $B_c \rightarrow J/\psi \pi \rightarrow \mu^+ \mu^- \pi$ and $B_c \rightarrow J/\psi \pi \rightarrow e^+ e^- \pi$ are feasible, and the events are presented in Table 4, in which we considered the quark mass dependence.

At last, let us study some certain channels which have been measured by the LHCb collaboration recently. The LHCb collaboration have measured $Br(B_c^+ \rightarrow J/\psi \pi^+ \pi^- \pi^+)/Br(B_c^+ \rightarrow J/\psi \pi^+)$ to be $2.41 \pm 0.30 \pm 0.33$, using 0.8fb^{-1} data of pp collisions at center-of-mass energy $\sqrt{s} = 7\text{TeV}$ [8]. Experimentally the reconstructed invariant mass distribution of the $\pi^+ \pi^- \pi^+$ combinations favors a resonance state $a_1^+(1260)$.

In theoretical aspects, there are mainly two channels: $B_c^+ \rightarrow J/\psi a_1^+(1260)$ followed with $a_1^+(1260) \rightarrow \pi^+ \pi^- \pi^+$; and $B_c^+ \rightarrow \Psi(2S) \pi^+$ with $\Psi(2S) \rightarrow J/\psi \pi^+ \pi^-$ which contribute to the signal of $B_c^+ \rightarrow J/\psi \pi^+ \pi^- \pi^+$. Practically, $Br(B_c^+ \rightarrow \Psi(2S) \pi^+)/Br(B_c^+ \rightarrow J/\psi \pi^+) = (A_0^2(0)_{\Psi(2S)} (m_{B_c}^2 - m_{\Psi(2S)}^2)^3) / (A_0^2(0)_{\Psi} (m_{B_c}^2 - m_{\Psi}^2)^3) \approx 0.26$, and $Br(\Psi(2S) \rightarrow J/\psi \pi^+ \pi^-) = 33.6\%$ [39]. So the contribution to $Br(B_c^+ \rightarrow J/\psi \pi^+ \pi^- \pi^+)/Br(B_c^+ \rightarrow J/\psi \pi^+)$ from $\Psi(2S)$ is 0.08, which explained the experiment data that favor the resonance state $a_1^+(1260)$ rather than $\Psi(2S)$.

In the former section, we have performed a complete QCD NLO calculation of B_c decays into S-wave charmonia and light mesons. And we found that the factorizable contribution account for more than 85% of total results at NLO accuracy in heavy quark limit as Eq. (44). Here we assume that it is also hold in $B_c^+ \rightarrow J/\psi a_1^+(1260)$, i.e. it can reserve a high-accuracy just considering the factorizable diagrams. So we adopt the naive factorization scheme. And for the axial-vector meson $a_1^+(1260)$, the matrix element for its creation is

$$\langle a_1^+(1260)(p, \epsilon^*) | \bar{u} \gamma_\mu \gamma_5 d | 0 \rangle = -i f_{a_1} m_{a_1} \epsilon_\mu^*. \quad (45)$$

Then we can obtain the ratio

$$\frac{Br(B_c^+ \rightarrow J/\psi a_1^+(1260))}{Br(B_c^+ \rightarrow J/\psi \pi^+)} = \frac{f_{a_1}^2 \lambda_0}{f_\pi^2 A_0^2(0)} [\lambda_1 A_1^2(m_{a_1}^2) + \lambda_2 A_2^2(m_{a_1}^2) + \lambda_3 A_1(m_{a_1}^2) A_2(m_{a_1}^2) - \lambda_4 V^2(m_{a_1}^2)],$$

with

$$\lambda_0 = \frac{\sqrt{(m_{a_1}^2 + m_{B_c}^2 - m_\psi^2)^2 - 4m_{a_1}^2 m_{B_c}^2}}{4m_\psi^2 (m_{B_c} + m_\psi)^2 (m_{B_c}^2 - m_\psi^2)^3}, \quad (46)$$

Table 3: Branching ratios (in %) of exclusive non-leptonic B_c decays into S-wave charmonium states. For the lifetime of the B_c we take $\tau(B_c) = 0.453$ ps. In our work, we choose the quantities $m_c = 1.4$ GeV, $m_b = 4.9$ GeV, and $\mu = 3$ GeV. The uncertainty in the first column of the value is from varying the renormalization scale μ from 2.5 GeV to 5 GeV; while the uncertainty in the second column comes from varying the quark mass m_c/m_b from 1.5/4.8 to 1.3/5.0.

Mode	This work(NLO)	LO	[41, 42]	[43]	[44]	[45]	[46]	[47]	[48]	[49]
$B_c^+ \rightarrow \eta_c \pi^+$	$5.19^{+0.44+0.55}_{-1.01-0.34}$	2.95	2.0	2.2	1.3	0.26	0.85	1.4	1.9	2.1
$B_c^+ \rightarrow \eta_c \rho^+$	$14.5^{+1.29+1.53}_{-2.92-0.95}$	7.89	4.2	5.9	3.0	0.67	2.0	3.3	4.5	-
$B_c^+ \rightarrow \eta_c K^+$	$0.38^{+0.03+0.04}_{-0.07-0.02}$	0.21	0.13	0.17	0.13	0.02	0.06	0.11	0.15	-
$B_c^+ \rightarrow \eta_c K^{*+}$	$0.77^{+0.07+0.08}_{-0.16-0.05}$	0.41	0.20	0.31	0.21	0.04	0.11	0.18	0.25	-
$B_c^+ \rightarrow J/\psi \pi^+$	$2.91^{+0.15+0.40}_{-0.42-0.27}$	2.22	1.3	2.1	0.73	1.3	0.61	1.1	1.7	2.0
$B_c^+ \rightarrow J/\psi \rho^+$	$8.08^{+0.45+1.09}_{-1.21-0.73}$	6.03	4.0	6.5	2.1	3.7	1.6	3.1	4.9	-
$B_c^+ \rightarrow J/\psi K^+$	$0.22^{+0.01+0.03}_{-0.03-0.02}$	0.16	0.11	0.16	0.07	0.07	0.05	0.08	0.13	-
$B_c^+ \rightarrow J/\psi K^{*+}$	$0.43^{+0.02+0.06}_{-0.07-0.04}$	0.32	0.22	0.35	0.16	0.20	0.10	0.18	0.28	-
$B_c^+ \rightarrow \psi(2S)\pi^+$	$0.76^{+0.04+0.10}_{-0.11-0.07}$	0.58	-	0.27	-	0.19	0.11	-	-	-
$B_c^+ \rightarrow \psi(2S)\rho^+$	$2.11^{+0.12+0.28}_{-0.32-0.19}$	1.57	-	0.77	-	0.48	0.18	-	-	-
$B_c^+ \rightarrow \psi(2S)K^+$	$0.057^{+0.003+0.008}_{-0.008-0.005}$	0.042	-	0.019	-	0.009	0.01	-	-	-
$B_c^+ \rightarrow \psi(2S)K^{*+}$	$0.112^{+0.005+0.015}_{-0.018-0.010}$	0.083	-	0.041	-	0.026	0.01	-	-	-

Table 4: The events of $B_c \rightarrow J/\psi \pi \rightarrow \mu^+ \mu^- \pi$, $B_c \rightarrow J/\psi \pi \rightarrow e^+ e^- \pi$ and $B_c \rightarrow \eta_c \pi \rightarrow \gamma \gamma \pi$ with 10fb^{-1} data, using various values of the c -quark mass m_c and fixed b -quark mass $m_b = 4.8$ GeV.

-	Tevatron ($\sqrt{S} = 2.$ TeV)					LHC ($\sqrt{S} = 14.$ TeV)				
m_c (GeV)	1.4	1.5	1.6	1.7	1.8	1.4	1.5	1.6	1.7	1.8
σ_{B_c} (nb)	13.4	10.5	8.48	6.89	5.63	214	160	139	114	95.1
$\mu^+ \mu^- \pi$ ($\times 10^4$)	2.54	2.15	1.79	1.56	1.40	40.6	32.8	29.3	25.9	23.6
$e^+ e^- \pi$ ($\times 10^4$)	2.54	2.15	1.79	1.57	1.40	40.6	32.8	29.3	26.0	23.7
$\gamma \gamma \pi$	47	37	32	27	24	754	567	525	459	413

$$\lambda_1 = (m_{B_c} + m_\psi)^4 (-2m_{a_1}^2 (m_{B_c}^2 - 5m_\psi^2) + m_{a_1}^4 + (m_{B_c}^2 - m_\psi^2)^2), \quad (47)$$

$$\lambda_2 = (-2m_{a_1}^2 (m_{B_c}^2 + m_\psi^2) + m_{a_1}^4 + (m_{B_c}^2 - m_\psi^2)^2)^2, \quad (48)$$

$$\lambda_3 = 2(m_{B_c} + m_\psi)^2 (m_{a_1}^2 - m_{B_c}^2 + m_\psi^2) (m_{a_1}^2 - (m_{B_c} - m_\psi)^2) (m_{a_1}^2 - (m_{B_c} + m_\psi)^2), \quad (49)$$

$$\lambda_4 = -8m_{a_1}^2 m_\psi^2 (-2m_{a_1}^2 (m_{B_c}^2 + m_\psi^2) + m_{a_1}^4 + (m_{B_c}^2 - m_\psi^2)^2). \quad (50)$$

According to the Ref. [50], we assume $Br(a_1^+(1260) \rightarrow \pi^+ \pi^- \pi^+)$ is equal $Br(a_1^+(1260) \rightarrow \pi^+ \pi^0 \pi^0)$ and its value is 50%. And we take the input parameters $f_{a_1} = 0.23\text{GeV}$ from the QCD sum rules [51], $m_{a_1} = 1.23\text{GeV}$ from the Particle Data Group [39]. The final result is

$$\frac{Br(B_c^+ \rightarrow J/\psi \pi^+ \pi^- \pi^+)}{Br(B_c^+ \rightarrow J/\psi \pi^+)} = 2.75^{+0.03+0.22}_{-0.04-0.05},$$

The uncertainties of our result come from the renormalization scale and quark mass. It is compatible with the experimental data $2.41 \pm 0.30 \pm 0.33$ when considering its uncertainty.

Table 5: Branching fraction ratio in comparison with the LHCb's data.

Ratio	our work	LHCb
$Br(B_c^+ \rightarrow J/\psi \pi^+ \pi^- \pi^+)/Br(B_c^+ \rightarrow J/\psi \pi^+)$	2.75	$2.41 \pm 0.30 \pm 0.33$ [8]
$Br(B_c^+ \rightarrow J/\psi K^+)/Br(B_c^+ \rightarrow J/\psi \pi^+)$	0.075	$0.069 \pm 0.019 \pm 0.005$ [9]
$Br(B_c^+ \rightarrow \Psi(2S)\pi^+)/Br(B_c^+ \rightarrow J/\psi \pi^+)$	0.260	$0.250 \pm 0.068 \pm 0.014 \pm 0.006$ [10]
$Br(B_c^+ \rightarrow \Psi(2S)K^+)/Br(B_c^+ \rightarrow J/\psi \pi^+)$	0.02	-
$Br(B_c^+ \rightarrow J/\psi \rho^+)/Br(B_c^+ \rightarrow J/\psi \pi^+)$	2.77	-
$Br(B_c^+ \rightarrow J/\psi K^{*+})/Br(B_c^+ \rightarrow J/\psi \pi^+)$	0.147	-

In order to conveniently compare with the LHCb's data, we present our prediction and experimental data in Table 5. For the former three channel, our results can explain the data perfectly. While for the latter three channels, more data is needed to investigate the validity of NRQCD factorization on B_c decays .

5 Conclusions

We have performed a comprehensive NLO analysis for the B_c meson decays into S-wave charmonia and light mesons such as π , ρ , K and K^* . The NLO QCD correction provides a large K factor which substantially enhance the branching ratio, while the μ dependence is reduced corresponding. Considering about uncertainties of sorts of input parameters, we find out the largest uncertainty comes from the masses of bottom and charm quarks.

In the heavy quark limit, the analytic amplitude up to NLO accuracy is derived. Therein logarithm $\ln z$ with $z = m_c/m_b$ is absent in the contribution for color-singlet operator, while this kind of logarithm and double logarithm $\ln^2 z$ emerge in that of color-octet operator. And the result of asymptotic NLO where we only reserve the leading order in the z expansion can account for more than 85% of the complete NLO's result in which z is fixed to its physical value. Therefor it is enough to use the asymptotic formulas for phenomenological studies at NLO accuracy.

Numerical results show that the latest LHCb's data on B_c decays can be explained perfect using NRQCD factorization under their corresponding uncertainties. We also predicted another three channels which shall be checked in the upcoming data. The large branching ratio and the clear signal of final states make it reliable for the measurement of the absolute branching ratios for the processes $B_c \rightarrow J/\psi \pi$, $B_c \rightarrow J/\psi \rho$ and $B_c \rightarrow J/\psi K$ within the updated LHCb's data.

Acknowledgement

This work was supported in part by the National Natural Science Foundation of China(NSFC) under the grants 10935012, 10821063 and 11175249.

Appendix

A LCDA for light mesons and projection operators for heavy quarkonia

Considering the twist-2 and twist-3 light-cone distribution amplitudes for Pion, we have the matrix element of quarks hadronization projection operator [17, 23]

$$\bar{u}_{\alpha a}(xP)\Gamma(x, \dots)_{\alpha\beta, ab, \dots} v_{\beta b}(\bar{x}P) \longrightarrow \frac{if_\pi}{4N_c} \int_0^1 dx M^\pi(x)_{\alpha\beta} \Gamma(x, \dots)_{\alpha\beta, aa, \dots}, \quad (51)$$

with the decay constant $f_\pi = 130.4\text{MeV}$, $\bar{x} = 1 - x$ and

$$M^\pi(x)_{\alpha\beta} = \left\{ \not{P}\gamma_5 \phi(x) - \mu_\pi \gamma_5 \left(\phi_p(x) - i\sigma_{\mu\nu} n_-^\mu v^\nu \frac{\phi'_\sigma(x)}{6} + i\sigma_{\mu\nu} P^\mu \frac{\phi_\sigma(x)}{6} \frac{\partial}{\partial k_{\perp\nu}} \right) \right\}_{\alpha\beta}, \quad (52)$$

here $\mu_\pi = m_\pi^2/(m_u + m_d)$, n_\pm are light cone vectors, $\phi(x)$ is twist-2 distribution amplitude and $\phi_p(x)$ and $\phi_\sigma(x)$ are twist-3 ones. For Pion, up to twist-2 [17, 53]

$$\phi_\pi(x) = 6x\bar{x}\{1 + a_1 C_2^{3/2}(\bar{x} - x) + a_2 C_4^{3/2}(\bar{x} - x)\}, \quad (53)$$

with $a_1 = 0.44$, $a_2 = 0.25$, and the Gegenbauer polynomials are defined by

$$C_2^{3/2}(z) = \frac{3}{2}(5z^2 - 1), \quad C_4^{3/2}(z) = \frac{15}{8}(21z^4 - 14z^2 + 1). \quad (54)$$

Then, for vector meson ρ , the corresponding matrix element of hadronization projection operator is [17, 23]

$$\bar{u}_{\alpha a}(xP')\Gamma(x, \dots)_{\alpha\beta, ab, \dots} v_{\beta b}(\bar{x}P') \longrightarrow \frac{if_\rho}{4N_c} \int_0^1 dx M^\rho(x)_{\alpha\beta}\Gamma(x, \dots)_{\alpha\beta, aa, \dots}, \quad (55)$$

$$M_{\alpha\beta}^\rho = M_{\alpha\beta\parallel}^\rho + M_{\alpha\beta\perp}^\rho, \quad (56)$$

with

$$M_{\parallel}^\rho = -\frac{if_\rho}{4} \frac{m_\rho(\varepsilon^* \cdot n_+)}{2E} E \not{n}_- \phi_{\parallel}(u) - \frac{if_{\perp} m_\rho}{4} \frac{m_\rho(\varepsilon^* \cdot n_+)}{2E} \left\{ -\frac{i}{2} \sigma_{\mu\nu} n_-^\mu n_+^\nu h_{\parallel}^{(t)}(u) - iE \int_0^u dv (\phi_{\perp}(v) - h_{\parallel}^{(t)}(v)) \sigma_{\mu\nu} n_-^\mu \frac{\partial}{\partial k_{\perp\nu}} + \frac{h_{\parallel}^{(s)}(u)}{2} \right\} \Big|_{k=up'}, \quad (57)$$

and

$$M_{\perp}^\rho = -\frac{if_{\perp}}{4} E \not{\varepsilon}_\perp^* \not{n}_- \phi_{\perp}(u) - \frac{if_\rho m_\rho}{4} \left\{ \not{\varepsilon}_\perp^* g_{\perp}^{(v)}(u) - E \int_0^u dv (\phi_{\parallel}(v) - g_{\perp}^{(v)}(v)) \not{n}_- \varepsilon_{\perp\mu}^* \frac{\partial}{\partial k_{\perp\mu}} + i\varepsilon_{\mu\nu\rho\sigma} \varepsilon_{\perp}^{*\nu} n_-^\rho \gamma^\mu \gamma_5 \left[n_+^\sigma \frac{g_{\perp}^{(a)}(u)}{8} - E \frac{g_{\perp}^{(a)}(u)}{4} \frac{\partial}{\partial k_{\perp\sigma}} \right] \right\} \Big|_{k=up'}. \quad (58)$$

Up to twist-2, the LCDA for longitudinally polarized ρ meson is

$$\phi_{\rho, \parallel}(x) = 6x\bar{x}\{1 + a_1^\rho C_2^{3/2}(\bar{x} - x)\}, \quad (59)$$

here $a_1^\rho = 0.18$.

In addition the twist-2 LCDA for K meson is [53]

$$\phi_K(x) = 6x\bar{x}\{1 + 0.51(\bar{x} - x) + 0.2C_2^{3/2}(\bar{x} - x)\}, \quad (60)$$

and for longitudinally polarized K^* meson

$$\phi_{K^*, \parallel}(x) = 6x\bar{x}\{1 + 0.57(\bar{x} - x) + 0.07C_2^{3/2}(\bar{x} - x)\}, \quad (61)$$

At last, using leading Fock states for heavy quarkonium, the quarks hadronization projection operators are [22]

$$\begin{aligned} v(p_b)\bar{u}(p_c) &\longrightarrow \frac{1}{2\sqrt{2}}\gamma_5(\not{P}_{B_c} + m_b + m_c) \times \left(\frac{1}{\sqrt{\frac{m_b+m_c}{2}}}\psi_{B_c}(0) \right) \otimes \left(\frac{\mathbf{1}_c}{\sqrt{N_c}} \right), \\ v(p_{\bar{c}})\bar{u}(p_c) &\longrightarrow \frac{1}{2\sqrt{2}} \not{\varepsilon}(\not{P}_{\Psi} + m_c + m_c) \times \left(\frac{1}{\sqrt{\frac{m_c+m_c}{2}}}\psi_{\Psi}(0) \right) \otimes \left(\frac{\mathbf{1}_c}{\sqrt{N_c}} \right). \end{aligned} \quad (62)$$

The NLO Schrödinger wave function at origin of J/ψ is determined by leptonic decay width

$$|\psi_{J/\psi}(0)|^2 = \frac{m_{J/\psi}^2}{16\pi\alpha^2 e_c^2} \frac{\Gamma(J/\psi \rightarrow e^+ e^-)}{(1 + \pi\alpha_s C_F/v - 4\alpha_s C_F/\pi)}. \quad (63)$$

B Renormalization and infre-red subtractions

The renormalization constants include Z_2 , Z_3 , Z_m , and Z_g , corresponding to heavy quark field, gluon field, quark mass, and strong coupling constant g , respectively. Here, in our calculation the Z_g is defined in the modified-minimal-subtraction ($\overline{\text{MS}}$) scheme, while for the other three the on-shell (OS) scheme is adopted, which tells

$$\begin{aligned} \delta Z_m^{OS} &= -3C_F \frac{\alpha_s}{4\pi} \left[\frac{1}{\epsilon_{UV}} - \gamma_E + \ln \frac{4\pi\mu^2}{m^2} + \frac{4}{3} + \mathcal{O}(\epsilon) \right], \\ \delta Z_2^{OS} &= -C_F \frac{\alpha_s}{4\pi} \left[\frac{1}{\epsilon_{UV}} + \frac{2}{\epsilon_{IR}} - 3\gamma_E + 3 \ln \frac{4\pi\mu^2}{m^2} + 4 + \mathcal{O}(\epsilon) \right], \\ \delta Z_3^{OS} &= \frac{\alpha_s}{4\pi} \left[(\beta_0 - 2C_A) \left(\frac{1}{\epsilon_{UV}} - \frac{1}{\epsilon_{IR}} \right) + \mathcal{O}(\epsilon) \right], \\ \delta Z_g^{\overline{\text{MS}}} &= -\frac{\beta_0}{2} \frac{\alpha_s}{4\pi} \left[\frac{1}{\epsilon_{UV}} - \gamma_E + \ln 4\pi + \mathcal{O}(\epsilon) \right]. \end{aligned} \quad (64)$$

While for light quark such as u and d quarks, the corresponding renormalization constant is

$$\delta Z_2^{OS} = -C_F \frac{\alpha_s}{4\pi} \left(\frac{1}{\epsilon_{UV}} - \frac{1}{\epsilon_{IR}} \right). \quad (65)$$

On above, $\delta Z_i = Z_i - 1$, and $\beta_0 = (11/3)C_A - (4/3)T_f n_f$ is the one-loop coefficient of the QCD beta function; $C_A = 3$ and $T_F = 1/2$ attribute to the SU(3) group; μ is the renormalization scale.

We write the renormalized operator matrix elements as [25]

$$\langle Q_i \rangle_{\text{ren}} = Z_\psi \hat{Z}_{ij} \langle Q_j \rangle_{\text{bare}}, \quad (66)$$

where $i, j = 0, 8$ and $Z_\psi = Z_b^{1/2} Z_c^{1/2} Z_q$ contains the quark field renormalization factors of the massive b-quark Z_b , the massive c-quark Z_c and the massless quarks Z_q , whereas \hat{Z} is the operator renormalization matrix in the effective theory. It reads

$$\hat{Z} = 1 + \begin{pmatrix} 0 & 6 \\ \frac{4}{3} & -2 \end{pmatrix} \frac{\alpha_s}{4\pi} \frac{1}{\epsilon}. \quad (67)$$

All of soft IR divergences are canceled when summing them up, and Coulomb divergences can be canceled by the corresponding counter-term from the NLO Schrödinger wave function at origin. While the left collinear divergences can be removed by Pion wave function's subtraction [54].

C Formulas for non-factorizable contribution

In this subsection, the asymptotic formulas for one loop non-factorizable contribution are presented, where x is the collinear quark's momentum fraction in Pion and $z = m_c/m_b$ is the mass ratio for charm quark and bottom quark. The results are valid in heavy quark limit.

$$\begin{aligned} T_{\text{nf},0,x}^{(1)}(\eta_c) &= \phi_\pi(x) \left\{ \frac{2}{x} \ln \left(\frac{m_b^2}{\mu^2} \right) + \frac{2(x-1)\ln^2(x)}{3x(2x-1)} - \frac{2(\text{Li}_2(\frac{x-1}{x}) - \text{Li}_2(\frac{x}{x-1}))}{3x} \right. \\ &\quad - \frac{1}{3(x-1)x(2x-1)} f_1 - \frac{1}{3x(2x-1)} f_2 + \frac{1}{3(2x-1)^3} f_3 + \frac{1}{3(x-1)x(2x-1)^3} f_4 \\ &\quad \left. + \frac{1}{3x^2(2x-1)^3} f_5 + \frac{1}{3(x-1)x^2(2x-1)^3} f_6 \right\}, \end{aligned} \quad (68)$$

$$T_{\text{nf},0,x}^{(1)}(\Psi) = T_{\text{nf},0,x}^{(1)}(\eta_c), \quad (69)$$

with

$$\begin{aligned}
f_1 &= 2(x^2(\ln(2) - 4) - x(2 + 2\ln(2)) + 2 + \ln(2)) \ln(x + 1), \\
f_2 &= 2(x - 1)(-\text{Li}_2(\frac{x+1}{2x^2}) + \text{Li}_2(-\frac{1}{2x}) + 2\text{Li}_2(\frac{1}{x}) - \text{Li}_2(-2x) + \text{Li}_2(2(x+1))), \\
f_3 &= 8(x-1)^2(\text{Li}_2(4-2x) + 2\text{Li}_2(\frac{1}{1-x}) - \text{Li}_2(-\frac{x-2}{2(x-1)^2}) + \text{Li}_2(\frac{1}{2(x-1)}) - \text{Li}_2(2x-2)), \\
f_4 &= \ln(x)(-4(2x^2 - 3x + 1)^2 \ln(x+1) - 8x(x-1)^3 \ln(2-x) + 3 + 6\ln(2) \\
&\quad + x(2x(2x(-2x + 2(5x - 14)) \ln(2) - 3) + 15 + 56\ln(2)) - 17 - 46\ln(2)), \\
f_5 &= \ln(1-x)(x(x(4x(x-10x\ln(2)) + 5 + 18\ln(2)) - 37 - 38\ln(2)) + 19 + 4\ln(2)) \\
&\quad + 2(x-1)x(\ln(x+1) + 4(x-1)x(2\ln(2-x) + \ln(x+1))) - 3), \\
f_6 &= -8x^2(x-1)^3 \ln^2(1-x) + (x-1)(x(x(x^2(20 + 8\ln(2)) - x(72 + 16\ln(2)) \\
&\quad + 79 + 8\ln(2)) - 32) + 4) \ln(2-x) + x(2x(2x(28x^2 - 58x + 45) - 31) \\
&\quad + \pi^2(x-1)^2 + x(103 - 2x(6x(6x-13) + 83)) \ln(2) + 8 - 33\ln(2)) + 4\ln(2). \\
T_{8,nf,x}^{(1)}(\eta_c) &= \phi_\pi(x) \left\{ \frac{-11C_A + 48xN_c + 2n_f - 6}{9x} \ln\left(\frac{m_b^2}{\mu^2}\right) + \frac{9(x-1)\ln(z) - 5x + 2}{3(x-1)x} C_F - \frac{(3C_A - 1)\ln^2(z)}{18x} \right. \\
&\quad - \frac{2(-3\ln(z) + 5 + 3\ln(2))}{27x} n_f - \frac{\ln(z)}{54(x-1)x} ((138x - 144x\ln(2)) - 138 + 90\ln(2)) C_A + 144x \\
&\quad + 96x^2 \ln(1-x) - 96x^2 \ln(x) - 96x \ln(1-x) + 96x \ln(x) + 372x \ln(2) - 144 - 210\ln(2) \\
&\quad + \frac{1}{N_c} \left(\frac{2(\text{Li}_2(\frac{x-1}{x}) - \text{Li}_2(\frac{x}{x-1}))}{3x} - \frac{(x-2)(x(10x-11) + 2) \ln(1 - \frac{x}{2})}{3(1-2x)^2 x^2} \right) \\
&\quad + \frac{1}{3x(2x-1)} f_2 - \frac{1}{3(2x-1)^3} f_3 + \frac{1}{3(x-1)x(2x-1)^3} f_7 + \frac{1}{3x^2(2x-1)^3} f_8 + \frac{1}{3(x-1)x(2x-1)^3} f_9 \\
&\quad + C_A \left(-\frac{(2x+1)(\text{Li}_2(\frac{x-1}{x}) - \text{Li}_2(\frac{x}{x-1}))}{3x} - \frac{(x^2 \text{Li}_2(\frac{1-x}{2}) - x^2 \text{Li}_2(\frac{x}{2}) + 2x \text{Li}_2(\frac{x}{2}) - \text{Li}_2(\frac{1-x}{2}))}{(x-1)x} + \frac{1}{6x} f_2 \right. \\
&\quad - \frac{x-1}{3(2x-1)^3} f_3 + \frac{(-4x^2 + x-1)\ln(x)\ln(2x+1)}{3x(2x-1)} - \frac{(x-2)(3x-2)(8x^2 - 6x + 3)C_A \ln(1 - \frac{x}{2})}{6(1-2x)^2(x-1)x} \\
&\quad + \frac{\ln(x)}{6(x-1)x(2x-1)^3} f_{10} + \frac{\ln(1-x)}{6x^2(2x-1)^3} f_{11} - \frac{1}{6(x-1)x^2(2x-1)^3} f_{12} + \frac{1}{108(x-1)x^2(2x-1)^3} f_{13} \\
&\quad - \frac{(x^2 - x + 2)(\text{Li}_2(1-x) - \text{Li}_2(1 - \frac{x}{2}))}{9(x-1)x} + \frac{(x-3)(\text{Li}_2(x) - \text{Li}_2(\frac{x+1}{2}))}{9x} - \frac{3(x-2)\text{Li}_2(\frac{x}{2})}{x-1} \\
&\quad - \frac{7}{3} (\text{Li}_2(\frac{x-1}{x}) - \text{Li}_2(\frac{x}{x-1})) + \frac{3(x+1)\text{Li}_2(\frac{1-x}{2})}{x} + \frac{(x-2)(78x^2 - 51x - 2) \ln(1 - \frac{x}{2})}{18(x-1)x^2} \\
&\quad \left. + \frac{\ln(x)}{18(x-1)x} f_{14} + \frac{\ln(1-x)}{9(x-1)x^2} f_{15} + \frac{6}{108(x-1)x} f_{16} \right\}, \tag{70}
\end{aligned}$$

$$\begin{aligned}
T_{8,nf,x}^{(1)}(\Psi) &= T_{8,nf,x}^{(1)}(\eta_c) + \phi_\pi(x) \left\{ -\frac{16}{3} \ln\left(\frac{m_b^2}{\mu^2}\right) + \ln(z) \left(\frac{16(x-1)x \ln(1-x) - 16(x-1)x \ln(x) + 36x \ln(2) - 18\ln(2)}{9(x-1)x} \right. \right. \\
&\quad \left. - \frac{2(2x-1)\ln(2)C_A}{3(x-1)x} \right) + \frac{C_A}{18(x-1)x} f_{17} + \frac{1}{18(x-1)x} f_{18} \left. \right\}, \tag{71}
\end{aligned}$$

with

$$\begin{aligned}
f_7 &= \ln(x)(4(2x^2 - 3x + 1)^2 \ln(x+1) + (x+3)(2x-1)^3 + 8x(x-1)^3 \ln(2-x) \\
&\quad - 2(4x(x(5x-9) + 5) - 3)(x-1)\ln(2)), \\
f_8 &= \ln(1-x)(x(x(-4x(x+5) + 8x(5x-9)\ln(2) + 37 + 38\ln(2)) - 19 - 4\ln(2)) \\
&\quad + 2(x-1)x(-\ln(x+1) - 4(x-1)x(2\ln(2-x) + \ln(x+1))) + 3),
\end{aligned}$$

$$\begin{aligned}
f_9 = & 24x^3 \ln(2) \ln(4-2x) - 8x(x^3 + 3x - 1) \ln(2) \ln(2-x) + x(4x^3(13 \ln(2) - 28) - 8x^2(-29 + 3 \ln^2(2) + 8 \ln(2)) \\
& + 15x(\ln(2) - 12) + 62 + 8 \ln(2)) - \pi^2(x-1)^2 + 8x(x-1)^3 \ln^2(1-x) + 2x(x(-4(x-3)x - 13) + 6) \ln^2(x) \\
& - 2 \ln^2(x) + 4i\pi(x-1)^2 \ln(2) + (2x(x(x(4 \ln(2) - 16) + 8 - 12 \ln(2)) + 12 + 13 \ln(2)) \\
& - 2(5 + 3 \ln(2))) + 2 \ln(2) \ln(x+1) + 4 \ln(x+1) - 8 - 3 \ln(2),
\end{aligned}$$

$$\begin{aligned}
f_{10} = & (16x(x-1)^4 \ln(2-x) + 4(2x-1)^3(x-1)^2 \ln(x+1) - 2x(x-1)(2x(2x(4x-8-7 \ln(2)) + 10 + 17 \ln(2)) \\
& - 3(2+5 \ln(2))) + 2(1-2x)^2(x(4x-1)+1)(x-1) \ln(2x+1) + 1 + 2 \ln(2)),
\end{aligned}$$

$$\begin{aligned}
f_{11} = & (-32x^2(x-1)^3 \ln(2-x) - 2x(2x-1)^3(x-1) \ln(x+1) + x(x(4x(x(20x-37-20 \ln(2)) \\
& + 29 + 30 \ln(2)) - 51 - 52 \ln(2)) + 12 + \ln(16)) - 1),
\end{aligned}$$

$$\begin{aligned}
f_{12} = & (-(x-2)x(2x-1)(3x-2)(8x^2-6x+3) \ln(1-\frac{x}{2}) + \ln(1-x)(-32x^6 \ln(4-2x) \\
& + 32(2x(x(2x-3)+2)-1)x^2 \ln(2-x) + x(x(x(4x(x(4x(5+2 \ln(2)) - 57 \\
& - 20 \ln(2)) + 66 + 50 \ln(2)) - 167 - 172 \ln(2)) + 7(9+8 \ln(2))) - 13 - 4 \ln(2)) \\
& - 2(x-1)^2(2x-1)^3 x \ln(x+1) + 1) - 2(x-1)x(x(4x-1)+1)(1-2x)^2 \ln(x) \ln(2x+1)),
\end{aligned}$$

$$\begin{aligned}
f_{13} = & (x(6(x(x(72x^2-62x-23)+41)-13)(2x-1) \ln(2) + 8(47x-20)(2x-1)^3 - 3\pi^2(x(8x(x(20x-47)+39) \\
& - 101) + 8) + 36(x(2x(2x(2x(x+3)-17)+29)-23)+4) \ln^2(2)) + 18(16x^2(x-1)^4 \ln^2(1-x) \\
& + x((1-2x)^2((2x-1)(-6(x^2-1) \ln^2(\frac{x+1}{2}) + (-2(x-2)x-3) \ln^2(x) + 2(x-1)^2 \ln(2) \ln(x+1)) \\
& + 2(x((5-4x)x-2)+1) \ln(x) \ln(2x+1)) - (x-2)(3x-2)(8x^2-6x+3)(2x-1) \ln(1-\frac{x}{2}) \\
& + 6(x-2)x(2x-1)^3 \ln^2(1-\frac{x}{2})) + (x-1) \ln(1-x)(-32x^2(x-1)^3 \ln(2-x) \\
& - 2x(2x-1)^3(x-1) \ln(x+1) + x(x(4x(x(20x-37-20 \ln(2)) + 29 + 30 \ln(2)) - 51 \\
& - 52 \ln(2)) + 12 + 4 \ln(2)) - 1)) - 288x^2(x-1)^4 \ln(2) \ln(4-2x)),
\end{aligned}$$

$$\begin{aligned}
f_{14} = & (x(180x-58x \ln(2)-139+40 \ln(2)) - 2((x-1)x+2) \ln(1-x) + 2((x-1)x+2) \ln(2-x) \\
& + 64(x-1)x \ln(2x) - 2 - 4 \ln(2)),
\end{aligned}$$

$$\begin{aligned}
f_{15} = & (x(x^2 \ln(128x) - 32(x-1)x \ln(2-2x) + (3-4x) \ln(2x) - (x-3)(x-1) \ln(x+1)) \\
& + x(x(x(15+22 \ln(2)) - 9 - 28 \ln(2)) - 9) + 3),
\end{aligned}$$

$$\begin{aligned}
f_{16} = & (13 \ln(2)(\ln(32) - 6x^2) + x(384x - 380 + (19 - 117 \ln(2)) \ln(2)) + 20 - 30 \ln(2)) + 5\pi^2(12x - 7) \\
& + 6 \ln^2(x) - 324 \ln^2(\frac{x+1}{2}) + 6(64(x-1)x \ln^2(1-x) + 2x(-27(x-2) \ln^2(1-\frac{x}{2}) + 4(9-8x) \ln^2(x) \\
& + 27x \ln^2(\frac{x+1}{2})) - 2((x-1)x+2) \ln(2) \ln(2-x) + (2x((x-4) \ln(2) + 16) \\
& + 6 \ln(2)) \ln(x+1) + 192 \ln(x+1),
\end{aligned}$$

$$\begin{aligned}
f_{17} = & (-6(x-1)x \ln^2(1-x) + 6(x-1)x \ln^2(x) + 2(2x-1)(\pi^2 - 3 \ln^2(2)) \\
& + 24(x-1)x \ln(2) \ln(1-x) - 24(x-1)x \ln(2) \ln(x)),
\end{aligned}$$

$$\begin{aligned}
f_{18} = & 32(x-1)x \text{Li}_2(\frac{x-1}{x}) - 32(x-1)x \text{Li}_2(\frac{x}{x-1}) - 192x^2 - 46x^2 \ln^2(1-x) + 46x^2 \ln^2(x) \\
& + 64x^2 \ln(2-2x) \ln(1-x) - 72x^2 \ln(2) \ln(1-x) - 48x^2 \ln(1-x) + 72x^2 \ln(2) \ln(x) - 48x^2 \ln(x) \\
& - 64x^2 \ln(x) \ln(2x) - 10\pi^2 x + 160x + 46x \ln^2(1-x) - 46x \ln^2(x) + 28x \ln^2(2) - 64x \ln(2-2x) \ln(1-x) \\
& + 72x \ln(2) \ln(1-x) + 64x \ln(1-x) - 72x \ln(2) \ln(x) + 16x \ln(x) + 64x \ln(x) \ln(2x) \\
& + 8x \ln(2) \ln(2) - 44x \ln(2) - 16 \ln(1-x) + 4\pi^2 - 18 \ln^2(2) + 12 \ln(2) + 32 \ln(2).
\end{aligned}$$

References

- [1] N. Brambilla, et al. [Quarkonium Working Group], CERN-2005-005, [arXiv:hep-ph/0412158].
- [2] F. Abe, et al. [CDF Collaboration], Phys. Rev. Lett. **81**, 2432 (1998).
- [3] A. Abulencia et al. [CDF Collaboration], Phys. Rev. Lett. **97**, 012002(2006).
- [4] V. M. Abazov et al. [D0 Collaboration], Phys. Rev. Lett. **102**, 092001(2009).
- [5] T. Aaltonen et al. [CDF Collaboration], Phys. Rev. Lett. **100**, 182002(2008).
- [6] V. M. Abazov et al. [D0 Collaboration], Phys. Rev. Lett. **101**, 012001(2008).
- [7] R. Aaij et al. [LHCb Collaboration], Phys. Rev. Lett. **109**, 232001(2012).
- [8] R. Aaij et al. [LHCb Collaboration], Phys. Rev. Lett. **108**, 251802(2012).
- [9] R. Aaij *et al.* [LHCb Collaboration], JHEP **1309**, 075 (2013).
- [10] R. Aaij *et al.* [LHCb Collaboration], Phys. Rev. D **87**, 071103 (2013).
- [11] R. Aaij *et al.* [LHCb Collaboration], Phys. Rev. D **87**, 112012 (2013).
- [12] C.-H. Chang, C. Driouichi, P. Eerola and X.-G. Wu, Comput. Phys. Commun. **159**, 192 (2004).
- [13] C.-H. Chang, and X.-G. Wu, Eur. Phys. J. C**38**, 267-276 (2004).
- [14] Y.-N. Gao, J.-B. He, P. Robbe, M.-H. Schune, Z.-W. Yang, Chin. Phys. Lett. **27**, 061302(2010).
- [15] G. T. Bodwin, E. Braaten and G. P. Lepage, Phys. Rev. D **51**, 1125 (1995), [Erratum-
ibid.D55:5853,1997].
- [16] G. Buchalla, A. J. Buras and M. E. Lautenbacher, Rev. Mod. Phys, **68**, 1125 (1996).
- [17] M. Beneke, G. Buchalla, M. Neubert and C. T. Sachrajda, Nucl. Phys. B **591**, 313 (2000).
- [18] T. Hahn, Comput. Phys. Commun, **140**, 418 (2001).
- [19] R. Mertig, M. Böhm, and A. Denner, Comput. Phys. Commun, **4**, 345 (1991).
- [20] T. Hahn and M. Perez-Victoria, Comput. Phys. Commun, **118**, 153 (1999).
- [21] J.G. Körner, D. Kreimer and K. Schilcher, Z. Phys. C **54**, 503 (1992)
- [22] C.-F. Qiao, L.-P. Sun and R.-L. Zhu, JHEP **1108**, 131 (2011); L. -B. Chen, C. -F. Qiao and
R. -L. Zhu, Phys. Lett. B **726**, 306 (2013).
- [23] M. Beneke, Th. Feldmann, Nucl. Phys. B **592**, 3-34 (2001).
- [24] V.M. Braun and I.E. Filyanov, Z Phys. C **48**, 239 (1990).
- [25] Guido Bell, Ph.D. Thesis, arXiv:0705.3133[hep-ph].
- [26] G. Bell and T. Feldmann, JHEP **0804**, 061 (2008).
- [27] C.-F. Qiao, P. Sun and F. Yuan, JHEP **1208**, 087 (2012) .
- [28] C. -F. Qiao and R. -L. Zhu, Phys. Rev. D **87**, 014009 (2013).
- [29] R. Keith Ellis and Giulia Zanderighi, JHEP **0802**, 002 (2008).

- [30] Stefan Dittmaier, Nucl. Phys. B **675**, 447 (2003).
- [31] M. Beneke and S. Jager, Nucl. Phys. B **751** (2006) 160 [arXiv:hep-ph/0512351].
- [32] M. Beneke, G. Buchalla, M. Neubert and C. T. Sachrajda, Phys. Rev. Lett. **83** (1999) 1914.
- [33] M. Beneke, G. Buchalla, M. Neubert and C. T. Sachrajda, Nucl. Phys. B **591** (2000) 313.
- [34] J.P. Ma and Z.G. Si, Phys. Lett. B**647**, 419(2007).
- [35] Y. Jia and D. Yang, Nucl. Phys. B**814**, 217(2009).
- [36] M. Beneke and D. Yang, Nucl. Phys. B**736**,34-81 (2006).
- [37] Nikolai Kivel, JHEP **0705**, 019(2007).
- [38] Volker Pilipp, arXiv:0709.0497 [hep-ph].
- [39] K. Nakamura, et al, Particle Data Group, J. Phys. G **37**, 075021(2010).
- [40] E. J. Eichten and C. Quigg, Phys. Rev. D **49**, 5845-5856(1994).
- [41] V. V. Kiselev, A. E. Kovalsky and A. K. Likhoded, Nucl. Phys. B **585**, 353 (2000).
- [42] V. V. Kiselev, arXiv:hep-ph/0211021.
- [43] C. H. Chang and Y. Q. Chen, Phys. Rev. D **49**, 3399 (1994).
- [44] A. Y. Anisimov, P. Y. Kulikov, I. M. Narodetsky and K. A. Ter-Martirosian, Phys. Atom. Nucl. **62**, 1739 (1999).
- [45] P. Colangelo and F. De Fazio, Phys. Rev. D **61**, 034012 (2000).
- [46] D. Ebert, R. N. Faustov and V. O. Galkin, Phys. Rev. D **68**, 094020 (2003).
- [47] A. Abd El-Hady, J. H. Munoz and J. P. Vary, Phys. Rev. D **62**, 014019 (2000).
- [48] M. A. Ivanov, J. G. Körner, P. Santorelli, Phys. Rev. D **73**,054024 (2006).
- [49] Junfeng Sun, Dongsheng Du and Yueling Yang, Eur. Phys. J. C**60**, 107-117 (2009).
- [50] B. Aubert, et al. (BABAR Collaboration) Phys. Rev. Lett.**99**, 261801(2007).
- [51] K. C. Yang, Nucl. Phys. B**776**, 187(2007).
- [52] Hai-Yang Cheng and Sechul Oh, JHEP **1109**, 024 (2011); Guohuai Zhu, JHEP **1005**, 063 (2010).
- [53] Patricia Ball, V.M. Braun, Y. Koike and K. Tanaka, Nucl. Phys. B **529**, 323-382 (1998); C.-D. Lü, M.-Z. Yang, Eur.Phys.J. C **28**, 515-523 (2003).
- [54] E. Braaten, Phys. ReV. D**28**,524 (1983).